Observation of breather and soliton in a substituted polythiophene with a degenerate ground state

Takayoshi Kobayashi[*,1,2,3,4], **Juan Du**[**,1,2], **Wei Feng**[5], **Katsumi Yoshino**[6], **Sergei Tretiak**[7], **Avadh Saxena**[7], **and Alan R. Bishop**[7]

[1] Department of Applied Physics and Chemistry and Institute for Laser Science, University of Electro-communications, 1-5-1 Chofugaoka, Chofu, Tokyo 182-8585, Japan
[2] JST, ICORP, Ultrashort Pulse Laser Project, 4-1-8 Honcho, Kawaguchi, Saitama 332-0012, Japan
[3] Department of Electrophysics, National Chiao Tung University, 1001 Ta Hsueh Road, Hsin-Chu 3005, Taiwan
[4] Institute of Laser Engineering, Osaka University, 2-6 Yamada-Oka, Suita, Osaka 565-0871, Japan
[5] School of Materials Science and Engineering, Tianjin University, Tianjin 300072, P.R. China
[6] Shimane Institute for Industrial Technology, 1 Hokuryo-cho, Matsue, Shimane 690-0816, Japan
[7] Theoretical Division and Center for Nonlinear Studies, Los Alamos National Laboratory, Los Alamos, New Mexico 87545, USA

* Corresponding author: e-mail kobayashi@ils.uec.ac.jp, Phone: +81 424 435 845, Fax: +81 424 435 825
** e-mail dujuan@ils.uec.ac.jp, Phone: +81 424 435 846, Fax: +81 424 435 826

The ultrafast dynamics of a unique polythiophene derivative that has a degenerate ground state due to a quantum mechanical resonance was investigated using a sub-5-fs pulse laser. The method allowed us to study the electronic relaxation and vibrational dynamics in completely same conditions at the same time. The dynamics of a breather composed of a dynamic bound state of solitons generated immediately after photoexcitation was time-resolved to reveal coupling between the vibrational modes and the solitons. The C-C and C=C stretching modes were found to be modulated by the breather, whose lifetime was determined to be 30-50 fs. The results of quantum-chemical excited-state molecular dynamics simulation are consistent with experimental results. Our modeling results allow to identify related vibrational normal modes strongly coupled to the electronic degrees of freedom. Moreover, analysis of calculated trajectories of excited state shows appearance of short-lived breather excitation decaying due to intramolecular vibrational energy equilibration on a timescale of hundreds of femtoseconds, which also agrees well with the experimental results.
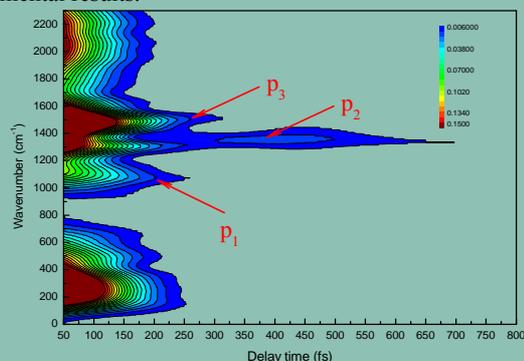
Contour maps of the two-dimensional Fourier power of the vibrational components obtained by spectrogram calculation for real-time data covering 680–690 nm

1 Introduction Soliton was first discovered in 1844 [1], which has been identified in many fields of nonlinear physics [2-7] including water waves, sound waves, matter waves, and electromagnetic waves [8]. According to simulations performed using the Su-Schrieffer-Heeger (SSH) Hamiltonian [9], a photogenerated electron-hole $(e-h)$ pair evolves into a soliton-antisoliton pair $(S-\bar{S})$ within 100 fs after photoexcitation because of barrier-free relaxation in a one-dimensional system. Matter-wave solitons have given rise to many interesting phenomena in the sim-

plest conducting polymer, *trans*-polyacetylene (*trans*-PA) [10], including anomalous conductivity and huge optical nonlinearity [11]. The formation times of solitons in polyacetylene have been determined to be <150 fs [12]. Even though the existence of a soliton in *trans*-PA is well known and has been extensively studied, besides *trans*-PA, there has been no other systematic study of conjugated polymer systems. This is probably because of the scarcity of polymers with a degenerate ground state.

The soliton pair is spatially localized to form a dynamic bound state called a breather, which has also been theoretically predicted [9, 13-16]. The excess energy of the photogenerated $(e-h)$ pair over that of the soliton pair induces collective carbon-carbon (C-C) oscillations, namely the breather mode, due to electron-phonon coupling. Breathers predicted in Ref. [17] have been observed in *trans*-PA [18], which was found to have a period of 44 fs and an extremely short lifetime of ~50 fs. However, there is not yet currently consensus among researchers as to whether breather is the primary photogenerated excitations and how they affect the ultrafast vibronic dynamics [18-23].

In the present work, the study of the dynamics of solitons and breather in a derivative of polythiophene which has a degenerate ground state (shown in Fig. 1(a)) has been reported. Polythiophene is one of the most promising materials for various device applications, which makes a detailed understanding of the dynamics of electronic state and vibrational dynamics photoexcitations in them and their derivatives highly desirable. In addition, there has been no other spectroscopic study of solitons except for *trans*-PA before, it is of great interest to study other degenerate-ground-state polymers' dynamics and compare any differences with *trans*-PA. To the best of our knowledge, this is the first observation of the existence of a breather and solitons and their dynamics in a system other than *trans*-PA. To rationalize the experimental data, we performed a quantum-chemical excited-state molecular dynamics simulation, and its results are consistent with experimental data, enabling breather excitations to be analyzed and related coupled vibrational normal modes to be identified.

2 Experimental descriptions In the present experiment, we utilized a nearly Fourier-transform limited visible-near-IR pulse generated from a noncollinear optical parametric amplifier (NOPA) seeded by a white-light continuum. The pump source of this NOPA system was a regenerative amplifier (Spectra Physics, Spitfire) with the following operating parameters: central wavelength, 800 nm; pulse duration, 50 fs; repetition rate, 5 kHz; average output power, 650 mW. We used a 1-mm-thick sapphire plate to generate the continuum spectrum. The NOPA output pulse was compressed with a pair of chirp mirrors and then with a prism pair, resulting in a nearly FT limited pulse duration of 6.3 fs Both the pump and probe pulses covered the spectral range extending from 515 to 716 nm [24], and the energies of them are about 50 and 6 nJ, re-

spectively. The pump probe signal at 128 different wavelengths was detected by a combined system of a polychromator and a multi-channel lock-in amplifier. Thanks to the extreme stability of the light source and noise reduction by the lock-in-detector, the time resolution is better than 1fs, which was recognized by the difference between the time resolved spectra at neighboring delay step obtained using the time-step of 0.2 fs.
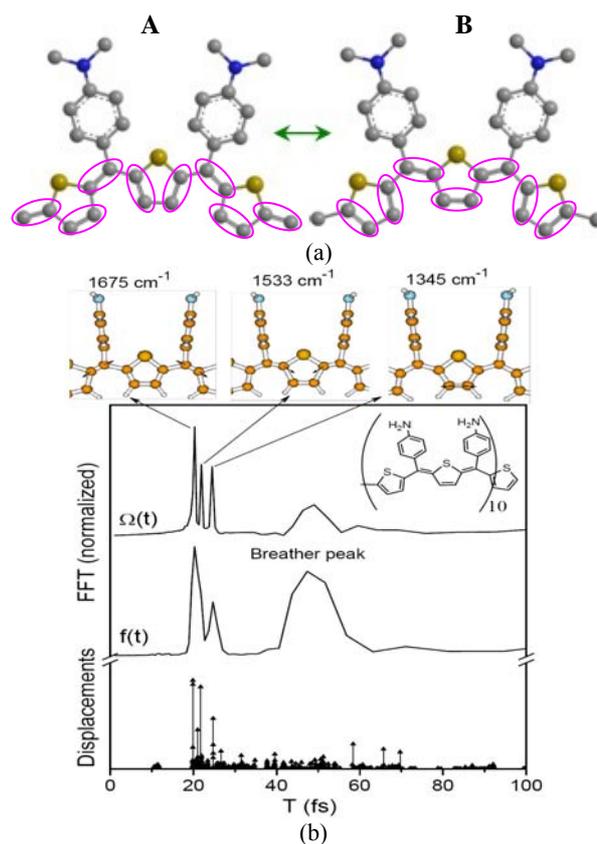
Figure 1 Two quantum mechanical resonant structures of (a) PHTDMABQ and (b) the excited state molecular dynamics simulations results. To make the degeneracy clearly, the pink elliptical circles denote the position of the C=C bond. (b) shows the normalized Fourier spectra of the lowest dipolar allowed excited state transition energy Ω(t) and its respective oscillator strength f(t) trajectories (top two plots), and the amplitudes of dimensionless displacements Δ (stick spectrum, bottom panel) along normal modes calculated in the oligomer with 10 repeat units, as shown in the inset. The three molecular structures at the top schematically show vibrational normal modes with frequencies strongly coupled to the electronic system, which lead to the formation of the breather excitation. These correspond to the C=C vibration and C-C stretches as schematically shown in the middle panel.

The sample studied in this study was a thin film of PHTDMABQ, whose structure is shown in our previous paper [25] and in Fig. 1(a). It was dissolved in methanol and cast on a quartz substrate for stationary and time-

resolved spectra measurements. All experiments were performed at room temperature (293±1 K).

3 Molecule structure The structure of PHTDMABQ is depicted in Fig. 1(a), whose monomer is a derivative of thiophene. It appears ostensibly not having a degenerate ground state; however, it has degeneracy due to the resonance of the inner structure of the polymer. In polythiophene, there is no degenerate ground state. After photoexcitation, bipolarons are generated. The two polarons in the bipolarons cannot be separated from each other because they are non degenerate. However, in the case of PHTDMABQ, there are two mesomeric forms to form a repeat unit. In each repeat unit, there are two thiophene rings with both cis and trans configurations. They can exchange their mesomeric structures without energy requirement. Therefore, the ground state structure can be either structure A or structure B as shown in Fig. 1(a). Because of the resonance of the internal structure of PHTDMABQ, it can have a degenerate ground state and thus solitons can be generated in it.

4 Quantum-chemical methodology To analyze the experimental data, we used the Austin Model 1 (AM1) Hamiltonian and an excited-state molecular dynamics (ESMD) computational package, which is described in detail in [26] and [27], to follow photoexcitation adiabatic dynamics on a picosecond timescale for all calculations presented in this study. The ESMD approach calculates the excited-state potential energy as $E_e(q) = E_g(q) + \Omega(q)$ in the space of nuclear coordinates q that span the entire (3N−6) dimensional space, where N is the total number of atoms in the molecule. Here, $\Omega(q)$ is the electronic transition frequency to the lowest $1B_u$ (band-gap) state of the photoexcited molecule. The program efficiently calculates analytical derivatives of $E_e(q)$ with respect to each nuclear coordinate q_i to evaluate forces and to subsequently step along the excited-state hypersurface using these gradients. All computations start from vertical excitation at the optimal ground-state molecular geometry. The total molecular energy $E_e(q)$ is conserved if no dissipative processes are included. Subsequent analysis of the photoexcited trajectories of the excitation energy $\Omega(q,t)$ and oscillator strength $f(q,t)$ in Fourier space allows us to identify periods of participating vibrational motions. Alternatively, the minimum of the excited state potential energy surface can be calculated by including an artificial dissipative force in the equations of motion corresponding to the relaxed excited-state geometry. To understand the formation of photoexcited breathers, we calculated the dynamics of the band-gap excited state in the 10-unit thiophene oligomer shown in the inset of Fig. 1(b), where the alkyl side-chain have been replaced by hydrohens, effectively reducing the molecular size for calculations. This molecule is sufficiently long (10 nm) compared to the characteristic exciton size of about 2 nm for the infinite chain limit to be valid.

5 Results and discussion

5.1 Electronic relaxation and molecular vibration dynamics In this paper the decay dynamics of the electronic state and vibrational dynamics highly correlated through excitonic coupling (vibronic coupling) were observed under the same condition at the same time. The real-time absorbance change signal $\Delta A(\omega)$ (Fig. 2a) shows the decay dynamics and spectral change associated with the change in the electronic state. On top of that signal the modulation $\delta\Delta A(\omega)$ of the $\Delta A(\omega)$ due to molecular vibration can be used to study the vibrational dynamics of the system completely in the same condition as that electronic dynamics study. This situation is difficult to be realized in experiment made by using conventional UV (VIS) pump-UV (VIS) probe experiment and time-resolved vibrational experiment.

(a)

(b)
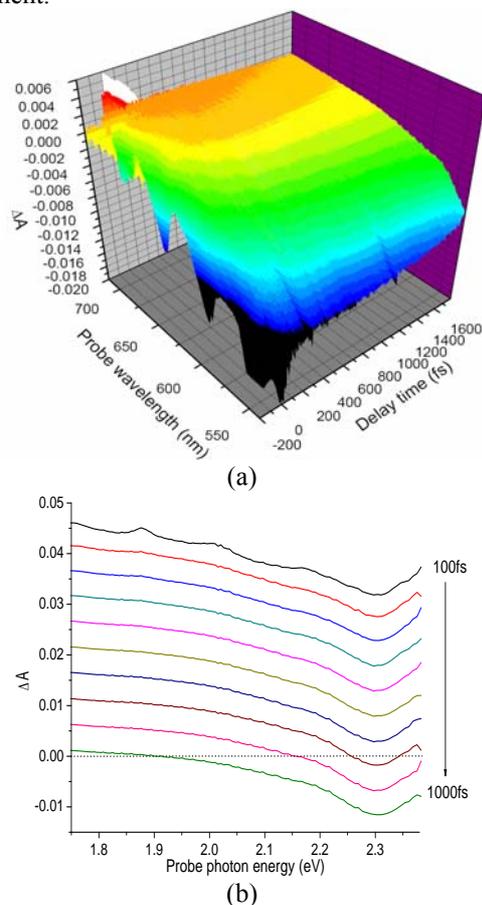
Figure 2 (a) Three-dimensional plot of the real-time absorbance change. (b) The time-resolved pump-probe spectra probed at 10 center delay time points from 100 to 1700 fs with an integration time width of 200 fs.

The difference absorbance (ΔA) signals in Fig. 2(a) exhibit oscillation due to molecular vibrations. As shown in the ΔA traces, the lifetimes of the electronic states consist of three components: 62±2 fs, 750±20 fs, and >3 ps27. The Fourier power spectra in Fig. 3 have peaks at 1111±7, 1343±7, and 1465±7 cm⁻¹ (p1, p2, and p3, respectively).

Phys. Status Solidi C **8**, No. 1 (2011)

77
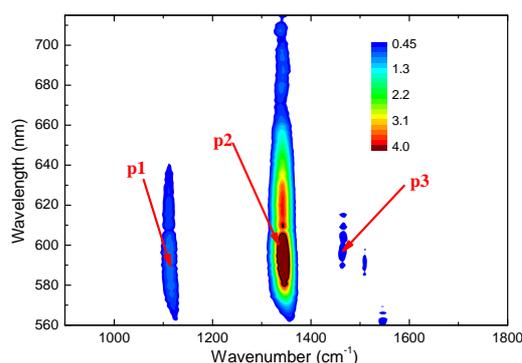
Figure 3 Fourier transform power spectra. The Fourier transform power spectrum at 615 nm is plotted as an example.

Theoretical calculations allow assigning these peaks to C-C stretching modes with different bond orders. Figure 1(b) shows the calculated dimensionless displacements Δ along the vibrational coordinates of the optimal geometries between the ground and excited states. This immediately enables us to identify the p1-p3 vibrational normal modes that are strongly coupled to the electronic excitation. These correspond to intra- and inter-thiophene ring C-C and C=C stretching motions (see Fig. 1(b), top structures). The highest, medium, and lowest frequencies are considered to correspond to C=C double bonds, a mixture of double and single bonds, and single bonds, respectively. The calculated vibrational frequencies (1345, 1533, and 1675 cm^{-1}) are overestimated by about 200 cm^{-1} compared to the experimental values, which is typical for semi-empirical calculations.

5.2 Dynamics of breather and soliton The requirement for the existence of solitons is a degenerate ground state structure. As mentioned before, PHTDMABQ has a degenerate ground state because the two quantum-mechanical resonance structures have equivalent energies. In Fig. 2(b), the transient absorption spectra exhibit negative absorbance changes in the photon energy range 1.91 to 2.38 eV, while for photon energies smaller than 1.91 eV, the absorbance change is positive. This increase in the absorbance is attributed to the tail of the solitons not fully relaxing to the band-gap center, as is the case in trans-PA [18]. Therefore, the induced absorption observed in poly-(substituted thiophene) is attributed to solitons. The positive value indicates the increased contribution of induced absorption due to a soliton with a peak near the mid gap, which is estimated to be around 1.4 eV.

Figure 4 shows the contour map obtained by the spectrogram analysis [28], which is suitable to study the dynamic process where the molecular geometrical relaxation or chemical reaction is accompanied with change in its vibrational frequency due to molecular structural change during the processes. As shown in Fig. 4, in addition to the three prominent peaks p1, p2, and p3, there are five more peaks appearing as side bands of p1-p3 at 270, 500, 640, 1960, and 2200 cm^{-1}. These five modes are breather modes

which are not visible in the two-dimensional Fourier power spectrum (Fig. 3) or in the stationary resonance Raman spectrum because they have extremely broad widths due to their short lifetimes. We also note that there are no detectable normal modes with substantial intensity in this spectral region coupled to the electronic excitation as evidenced by lack of significant displacements calculated in Fig. 1(b). The amplitudes of the high-frequency modes in the 2000-2200 cm^{-1} range decrease rapidly due to their short vibrational periods, which cannot be properly resolved by the finite pulse widths of both pump and probe pulses. However, the frequency is not affected and the breather excitation is clearly visible for the three sidebands with the lower frequencies.

The lifetimes of the side bands were determined to be about 50, 32, and 40 fs for sidebands of p1, p2, and p3, respectively. They are corresponding to the lifetime of the breather mode as observed decay time of 50fs in polyacetylene [18]. The theoretically predicted decay time is shorter than 100fs is again consistent with our observation. The result means the time for the breather mode to disappear followed by the separation into isolated solitons, and even shorter than that in polyacetylene. These short lifetimes are also corresponding to the shortest lifetime component of ~62 fs in the ΔA trace [25]. The ultrafast relaxation of ~50 fs of this nonlinear excitation ensures an ultrafast nonlinear response that can be used in all-optical switches.

The average frequency difference between the three main bands (1111, 1343, and 1465 cm^{-1}) and their corresponding side bands (270 and 1960cm^{-1} for 1111cm^{-1}, 500 and 2200cm^{-1} for 1343cm^{-1}, and 640cm^{-1} for 1465 cm^{-1}) is calculated to be 843±12 cm^{-1}, which is close to the experimentally observed value of about 760 cm^{-1} reported for polyacetylene [18], and theoretically expected values of 660-1000 cm^{-1} [14-17]. This frequency separation between the main bands and the satellite bands indicates that the breather modulates the C-C stretching modes with a period of ~40 fs generating the sidebands.

Consequently these sideband peaks appear due to nonlinear electron-vibrational excited state dynamics. To analyze these processes from theoretical calculations, we compute the power spectra of 750 fs photoexcited trajectories of the excitation energy $\Omega(q,t)$ and oscillator strength $f(q,t)$ shown in Fig. 1 (b) [26,29]. Both plots show an additional broad peak centered around 50 fs, corresponding to a vibration in the range 550 to 800 cm^{-1}, which does not correspond to any of the vibrational normal modes that exhibit substantial coupling to the electronic degrees of freedom (compare the displacements peaks with the FFT trajectories in Fig. 1(b)). Based on our previous computational studies, we assign this peak to a nonlinear breather excitation that occurs due to coupling of C-C vibrational motions. This vibrational excitation decays gradually over long time scales due to dissipation of vibrational energy to internal vibrational degrees of freedom that are weakly coupled to the electronic system; this is similar to previous findings

by us [26,29]. Power spectra of longer excited state trajectories (not shown) demonstrate diminishing breather peak. Our calculations estimate the breather lifetime to be about 0.2 ps without accounting for intermolecular dissipation channels (baths). Such fast decay is considered to be reasonably in agreement with our experiment data of ~50fs, in case we take into accounts of both intermolecular interactions and phonon energy leakage through the boundaries of conjugated segments (defects). These processes may reduce breather lifetime from 0.2 ps to ~50fs [29]. As expected, the breather peak is more pronounced in the power spectrum of the oscillator strength (see the inset of Fig. 4), since it is directly related to the modulation of the respective transition dipole moment [29].
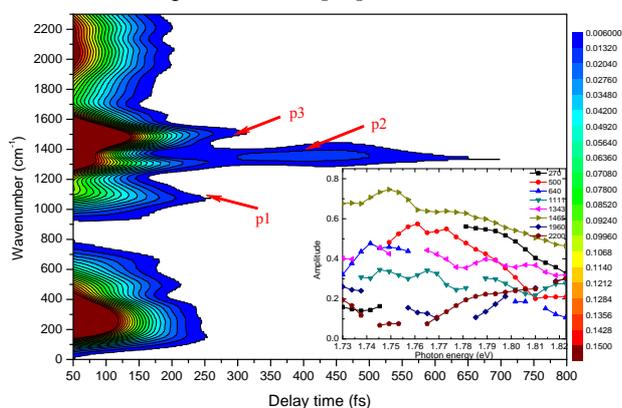
Figure 4 Contour maps of the two-dimensional Fourier power of the vibrational components obtained by spectrogram calculation for real-time data covering 680-690 nm (Inset is the probe photon energy dependence of the vibrational amplitude probed at a 110 fs gate delay time with a gate width of 120 fs (HWHM) in the spectrogram).

Thanks to the new multi-channel detection system developed we could observe the molecular vibration induced modulation $\delta\Delta A$ of the absorbance change ΔA at 128 different wavelengths simultaneously. In this way, the probe wavelength dependence can be used in detailed discussions on the photon energy dependence of modulation amplitudes of various modes. As shown in the inset of Fig. 4, the breather strongly contributes to the variations in the oscillator strength. Except for the modes at 1960 and 2200 cm^{-1}, the signal sizes of all the modes exhibit an almost monotonic increase when the photon energy is reduced from 1.82 to 1.73 eV. This is consistent with the theoretical discussion in Ref. [26]. The frequencies of these two modes are nearly equal to the overtones of 1111 cm^{-1}, which may affect the dynamics of the breather. Because both amplitude modulation (AM) and frequency modulation (FM) can affect the vibrational amplitude of the single and double C-C bonds [30], we also calculated the ratios of the amplitude of FM to that of AM; they were about 0.11 and 0.03 for the 1111 and 1343 cm^{-1} modes, respectively.

Similar feature is found for the positive absorbance change, as shown in Fig. 2(b). The magnitude of the positive absorbance change increases when the probe photon energy decreases. This provides the evidence of the larger contribution of the breather to the modulation ($\delta\Delta A$) of the difference absorbance change (ΔA) due to soliton in the lower energy range. We can interpret this feature in terms of the modulation of the transient spectrum of soliton by the vibrational modes as follows.

Molecular vibration associated with the breather and soliton is expected to modulate the transition energy and transition probability, and the amplitudes are expected to be proportional to the zeroth, first, and second derivatives of the absorption and/or stimulated emission spectrum depending on the mechanism of induction of the wavepacket motions [31]. Since the absorption spectrum of soliton is expected to be close to the mid gap, which is located at 1.4 eV in the case of polyacetylene, the spectral range of the present observation is higher energy tail of the soliton absorption as seen from the time-resolved spectrum as shown in Fig. 2(b). Therefore, all of the zeroth, first, and second derivatives of the absorption spectrum are expected to increase monotonically with decreasing probe photon energy.

Here we go back to the discussion of the above mentioned exceptional behavior of the probe wavelength dependence of the amplitudes of the two modes at 1960 and 2200 cm^{-1}. It can be explained in the following way. The molecular vibration modulates the transition probability and transition energy because of the electronic distribution change nearly instantaneously following the motion of nuclei during the molecular vibration. The frequencies of the modes at 1960 and 2200 cm^{-1} are nearly equal to the overtones of 1111 cm^{-1}, which may affect the dynamics of the breather. The electronic transition is modulated at periodically with period of ~30, 17 and 15 fs corresponding to the frequencies of 1111, 1960, and 2200 cm^{-1}, respectively. Then at integer multiple of about 32 fs all of them contribute. In case the vibrations of the modes are in phase or out of phase then the amplitudes of them may be affected by either constructive or destructive interference.

We now discuss the effect of the differences in the sizes and structures of the repeat units. The repeat unit in the *trans*-PA is composed of one single bond and one double bond, while in PHTDMABQ, it is more bulky since it has two thiophene rings with both *cis* and *trans* configurations (see Fig. 1). Since PHTDMABQ has a cis configuration in the thiophene ring, it is interesting to compare it with *cis*-PA. The lifetime of breather is expected to be longer than that in *trans*-PA. However, the decay time of the breather seems to be even shorter than that in *trans*-PA. That is because the lifetime is not determined by the separation of soliton pairs from the originally generated site in the polymer chain, but by the energy dissipation to internal vibrational freedom. Since PHTDMABQ has many more internal vibrational modes than *trans*-PA, its breather lifetime is even shorter than that of *trans*-PA.

6 Conclusions We investigated the ultrafast dynamics that take place immediately after excitation in a polythiophene derivative with a degenerate ground state.

The simulation results of quantum-chemical excited-state molecular dynamics agree reasonably well with the experimental data by showing formation of short-lived breather excitation. The breather lifetime was experimentally determined from the electronic spectral dynamics to be ~62 fs, which agrees with the time constants determined by the time-dependent signal intensity that appears as side peaks associated with the breather. Even though extensive theoretical studies have been conducted, to the best of our knowledge, this is the first time that modulation of the C-C single and double stretching modes by the breather have been experimentally observed other than in *trans*-PA.

References

[1] J. S. Russell, in: Report of the Fourteenth Meeting of the British Association for the Advancement of Science (Murray, London, 1844), pp. 311-390.

[2] N. S. Manton and P. Sutcliffe, Topological Solitons (Cambridge University Press, Cambridge, 2004).

[3] L. Khaykovich, F. Schreck, G. Ferrari, T. Bourdel, J. Cubizolles, L. D. Carr, Y. Castin, and C. Salomon, Science **296**, 1290 (2002).

[4] K. E. Strecker, G. B. Partridge, A. G. Truscott, and R. G. Hulet, Nature **417**, 150 (2002).

[5] M. Nakazawa, E. Yamada, and H. Kubota, Phys. Rev. Lett. **66**, 2625 (1991).

[6] W. P. Su, J. R. Schrieffer, and A. J. Heeger, Phys. Rev. Lett. **42**, 1698 (1979).

[7] A. M. Kosevich, B. A. Ivanov, and A. S. Kovalev, Phys. Rep. **194**, 117 (1990).

[8] G. I. Stegeman and M. Segev, Science **286**, 1518 (1999).

[9] W. P. Su and J. R. Schrieffer, Proc. Natl. Acad. Sci. USA **77**, 5626 (1980).

[10] H. Shirakawa, Rev. Mod. Phys. **73**, 713 (2001).

[11] H. Naarmann and N. Theophilou, Synth. Met. **22**, 1 (1987).

[12] C. V. Shank, R. Yen, R. L. Fork, J. Orenstein, and G. L. Baker, Phys. Rev. Lett. **49**, 1660 (1982).

[13] D. K. Campbell, Nature **432**, 455 (2004).

[14] M. Sasai and H. Fukutome, Prog. Theor. Phys. **79**, 61 (1988).

[15] S. R. Phillpot, A. R. Bishop, and B. Horovitz, Phys. Rev. B **40**, 1839 (1989).

[16] S. Block and H. W. Streitwolf, J. Phys.: Condens. Matter **8**, 889 (1996).

[17] A. R. Bishop, D. K. Campbell, P. S. Lomdahl, B. Horovitz, and S. R. Phillpot, Phys. Rev. Lett. **52**, 671 (1984).

[18] S. Adachi, V. M. Kobryanskii, and T. Kobayashi, Phys. Rev. Lett. **89**, 027401 (2002).

[19] G. S. Kanner, Z. V. Vardeny, G. Lanzani, and L. X. Zheng, Synth. Met. **116**, 71 (2001).

[20] T. Kobayashi, J. Du, W. Feng, K. Yoshino, S. Tretiak, A. Saxena, and A. R. Bishop, Phys. Rev. B **81**, 075205 (2009).

[21] K. M. Gaab and C. J. Bardeen, J. Phys. Chem. B **108**, 4619 (2004).

[22] G. Lanzani, G. Cerullo, C. Brabec, and N. S. Sariciftci, Phys. Rev. Lett. **90**, 047402 (2003).

[23] R. Lécuiller, J. Berréhar, C. Lapersonne-Meyer, and M. Schott, Phys. Rev. Lett. **80**, 4068 (1998).

[24] A. Baltuška, T. Fuji, and T. Kobayashi, Opt. Lett. **27**, 306.

[25] J. Du, Z. Wang, W. Feng, K. Yoshino, and T. Kobayashi, Phys. Rev. B **77**, 195205 (2008).

[26] S. Tretiak, A. Saxena, R. L. Martin, and A. R. Bishop, Proc. Natl. Acad. Sci. USA **100**, 2185 (2003).

[27] S. Tretiak, A. Saxena, R. L. Martin, and A. R. Bishop, Phys. Rev. Lett. **89**, 097402 (2002).

[28] M. J. J. Vrakking, D. M. Villeneuve, and A. Stolow, Phys. Rev. A **54**, R37 (1996).

[29] S. Tretiak, A. Piryatinski, A. Saxena, R. L. Martin, and A. R. Bishop, Phys. Rev. B **70**, 233203 (2004).

[30] T. Teramoto, Z. Wang, V. M. Kobryanskii, T. Taneichi, and T. Kobayashi, Phys. Rev. B **79**, 033202 (2009).

[31] T. Kobayashi, Z. Wang, and I. Iwakura, New J. Phys. **10**, 065009 (2008).